sustainability

MDPI

Article

Sawdust Recycling in the Development of Permeable Clay Paving Bricks: Optimizing Mixing Ratio and Particle Size

Md. Shafiquzzaman [1,*], Saad Mohammed A. Alqarawi [1], Husnain Haider [1], Md. Rafiquzzaman [2], Meshal Almoshaogeh [1], Fawaz Alharbi [1] and Yassine EL-Ghoul [3]

[1] Department of Civil Engineering, College of Engineering, Qassim University, Buraidah 51452, Saudi Arabia
[2] Department of Industrial Engineering and Management, Khulna University of Engineering and Technology, Khulna 9203, Bangladesh
[3] Department of Chemistry, College of Science, Qassim University, Buraidah 51452, Saudi Arabia
* Correspondence: M.UzzaMan@qu.edu.sa or shafiq@qec.edu.sa

Abstract: The permeable pavement system (PPS) has effectively contributed to stormwater management as a low-impact development (LID) technology. The suitability of clay bricks, consolidated with waste materials, for sustainable PPS applications in urban infrastructure needs further attention. In this study, several series of permeable clay paving bricks samples were prepared by mixing different ratios and particle sizes of sawdust (SD) with clay soil and firing at 900 °C. The raw soil and SD samples were characterized through sieve analysis, X-ray Fluorescence (XRF), X-ray diffraction (XRD), and Fourier-Transform Infrared Spectroscopy (FTIR). The bricks were tested for their compressive strength, bulk density, apparent porosity, water adsorption, permeability coefficient, and stormwater treatment efficiency. The clay soil comprised 17.5% clay/silt with appropriate amounts of SiO2 (50.47%), Al2O3 (19.14%), and fluxing agents (15.34%) and was suitable for brick manufacturing. XRD and FTIR analysis revealed that the soil predominantly comprises quartz, dolomite calcite, feldspar, kaolinite, illite, and chlorites. The SD samples were enriched with amorphous and crystalline cellulose. The compressive strength of the bricks decreased, while the permeability of the bricks increased with an increasing percentage of SD. An optimal percentage of 10% SD achieved a 21.2 MPa compressive strength and a 0.0556 m/s permeability coefficient, meeting the ASTM specifications for PPS. The optimal size of SD, between 0.5 and 1.0 mm, achieved the desired compressive strength of the bricks. The permeable bricks effectively removed the total suspended solids (TSS), turbidity, and BOD5 from the stormwater, which complies with the guidelines for wastewater reuse applications.

Keywords: permeable bricks; permeable pavements; clay soil; sawdust; compressive strength; permeability coefficient

Citation: Shafiquzzaman, M.; Alqarawi, S.M.A.; Haider, H.; Rafiquzzaman, M.; Almoshaogeh, M.; Alharbi, F.; EL-Ghoul, Y. Sawdust Recycling in the Development of Permeable Clay Paving Bricks: Optimizing Mixing Ratio and Particle Size. *Sustainability* **2022**, *14*, 11115. https://doi.org/10.3390/su141811115

Academic Editor: Jonathan Oti

Received: 2 August 2022
Accepted: 30 August 2022
Published: 6 September 2022

1. Introduction

Most arid and semi-arid countries, including Saudi Arabia, are fronting multifold climate-change-related challenges [1]. In addition, rapid urban development has caused a drastic loss in pervious surfaces, resulting in the insufficient infiltration of surface runoff and water pollution problems [2–4]. Even though the capacity of drainage infrastructure in these regions was designed for short-duration low-intensity rainfalls, in recent years, global climate change has increased the frequency of flash floods, resulting in significant environmental and economic loss in these regions [5]. Contemporary approaches, such as low-impact development (LID) and rainwater harvesting, are more resilient and are swiftly substituting conventional stormwater drainage schemes [6]. Utilizing natural and engineered infiltration and storage techniques, LID has proven to be a sustainable technique for achieving water balance for stormwater management [7–9]. LID essentially increases the pervious surfaces in urban areas to improve stormwater infiltration as well as the water quality through biological, chemical, and physical (filtration) processes [10,11].

Structural LID practices include but are not limited to: (a) bio-retention ponds, (b) green roofs, (c) permeable pavements, (d) infiltration trenches, (e) bio-swales, (f) rain barrels, (g) stormwater wetlands, and (d) sand filters [10].

Among the LID technologies, permeable pavement systems (PPSs) have been receiving considerable attention for the management of stormwater because of their unique properties for infiltrating stormwater on-site without covering space in the urban landscape [12]. PPS is a multilayer structure primarily consisting of several sub-base and base layers with a permeable surface on the top [13]. Acting as a stormwater reservoir, PPS has shown great potential in controlling flash floods by reducing the peak flow discharge and runoff volume through infiltration [14]. At the same time, the PPS is effective at removing various pollutants from the stormwater through filtration [15]. A previous study reported that PPS removes more than 70% of heavy metals and around 90% of hydrocarbons, while it retains 87% of the solids from surface runoff [16]. A modified PPS with grass swale can correspondingly reduce TSS, NO_3-N, NH_3-N, and TN up to 91%, 66%, 85%, and 42%, whereas heavy metals such as Cu, Fe, Pb, Mn, and Zn can be reduced by more than 75% [17]. A recent study by Shafiquzzaman et al. [18] reported that a PPS surface made of permeable clay bricks could reduce up to 99% TSS, 65–70% organics (BOD and COD), 70% NH_3-N, and 94% Pb from polluted stormwater.

Despite enormous progress, the effectiveness of the permeable clay bricks developed by a mix of various materials has yet to be investigated for sustainable applications in PSSs. Thus, further research on the quantitative and qualitative performance evaluation of PPSs is needed. Recent studies reported that the runoff infiltration capability and the pollutants removal efficacy of PPSs largely depend on the material properties of the PPS's surface [19]. Therefore, the surface layer needs to be carefully selected for the optimum performance of the PSS. Some studies focused on evaluating permeable asphalt-based and concrete-based pavements for runoff reduction and stormwater treatment [20,21]. The feasibility of PPS applications has also been tested in many recent studies, such as car parking areas, pedestrian pathways in light traffic areas, and smooth surfaces for low-speed vehicles [22,23]. These studies reported that the factors, including the properties of the materials used in the PPS layers, the setting of the layers, rainfall intensity, and rainfall duration, could impact the performance of the PPS [22,23]. Nevertheless, the selection of material compositions and PPS layer setting should be carefully considered for the PPS design to achieve the desired performance.

As a replacement for concrete and asphalt-based PPSs, a permeable clay brick pavement can be a sustainable alternative to urban stormwater management. Clay bricks made with simple technology can be implemented and achieve the goal of a low-cost LID. In past studies, various pore-forming waste materials were mixed with clay soil to produce environmentally-friendly permeable clay bricks [24–26]. To date, fly ash, rice husk, rice straw, sugarcane base waste, and many other waste materials from agricultural and industrial sources have been used to develop lightweight clay-based bricks [24–29]. Mixing these waste materials (5–30%) with soil generates pores in clay bricks. However, the applications of such clay bricks are restricted to building materials, such as wall and floor construction.

Among the waste materials, sawdust is considered to be one of the most abundant wastes produced by the wood/timber industry. More importantly, the average global wood harvesting rate has increased [30], and it is estimated that the industrial wood supply will increase by 55% by 2030 [31]. As a consequence, there are more concerns about sustainable methods for the disposal of sawdust, which is often burned off, causing environmental pollution [32]. Sawdust can be used as an alternative source of raw material in energy, agriculture, and manufacturing industries [32]. Several studies have investigated the application of sawdust-mixed fired clay bricks as building materials [33–35].

As per the authors' best knowledge, the application of SD in the manufacturing of permeable clay paving bricks has not been adequately studied in terms of their structural and hydrological properties [33]. The addition of SD to the clay mixture may be used as the pore-forming agent in the permeable bricks to achieve the desired permeability.

Nevertheless, the ratio and particle size of SD in the clay mixture may significantly decrease the desired strength of the bricks to be implemented in a PPS. Thus, the SD ratio and particle size in the porous clay bricks need further investigation into their structural, hydrological, and stormwater treatment performances. The present study aimed to develop a clay-based permeable brick made of soil and sawdust (SD) for light traffic and pedestrian applications in the urban areas of arid regions. Specifically, the study focused on optimizing the particle size and mixing ratio of SD by using the following optimization parameters of the clay bricks: compressive strength, bulk density, apparent porosity, water adsorption capacity, permeability coefficient, and stormwater treatment efficiency.

2. Materials and Methods

2.1. Clay Soil and Sawdust

The clay soil used for the manufacturing of the bricks was collected from the Najd Clay Brick Factory company located in the Unaizah district, AlQassim, Saudi Arabia. The soil samples were manually screened to remove straw, shells, and other impurities, ground with a hammer, and sieved through a 0.5 mm sieve. Figure 1a shows the soil samples used in this study. Sawdust was selected as the main pore-forming waste material for brick manufacturing. The primary reason for selecting SD was its frequent availability at a very low cost in the Gulf region. SD was collected from a carpenter shop of the local market in Unaizah, Al-Qassim. The collected SD was categorized into different particle sizes ranging from 0.5 mm to 1.5 mm by sieving through sieves of various sizes. Figure 1b shows an image of the sawdust used in this study.

Figure 1. Raw materials used for manufacturing the bricks, (**a**) clay soil, and (**b**) sawdust.

2.2. Porous Clay Bricks Manufacturing Process

The porous clay bricks were manufactured in the Environmental Engineering Laboratory, Department of Civil Engineering, College of Engineering, Qassim University. A conventional brick-making method presented in Figure 2 was employed to manufacture the porous clay bricks. All of the materials used for brick manufacturing were locally available in the Qassim region. Figure 3 shows the laboratory steps of the clay brick manufacturing procedure in this study. Making the bricks was initiated by weighing the soil and SD to the desired ratios using a digital balance. Different soil and SD ratios were well mixed to make a homogenous mixture (Figure 3a). Subsequently, tap water was slowly added to the mixture, and it was continually mixed to form the dough until achieving sufficient plasticity and workability (Figure 3b). The dough was then cast in a wooden mold with a standard size of 70 × 70 × 50 cm, which was adopted from previous studies (Figure 3c) [36,37]. All of the bricks were compacted using a manual press to ensure homogeneity and the desired

compaction. After casting, the bricks were left under room air for 24 h. Subsequently, the air-dried bricks were oven dried at 110 °C for 48 h. Alternatively, the bricks can also be dried under the sun to reduce energy costs. In the final steps, the oven-dried bricks were baked in a commercial furnace at Al-Fahad Construction Ltd. Uniazah, Al-Qassim, at 900 °C, with a gradually increasing temperature at a rate of 10 °C/min for 2.5 h. This firing temperature was selected based on the findings of past studies, which found that a firing temperature that ranged between 900 and 1000 °C is suitable for the manufacturing of clay bricks [38]. After baking, the bricks shown in Figure 3e,f were brought back to the laboratory and kept under water for 24 h for cleaning and curing before they were tested further.

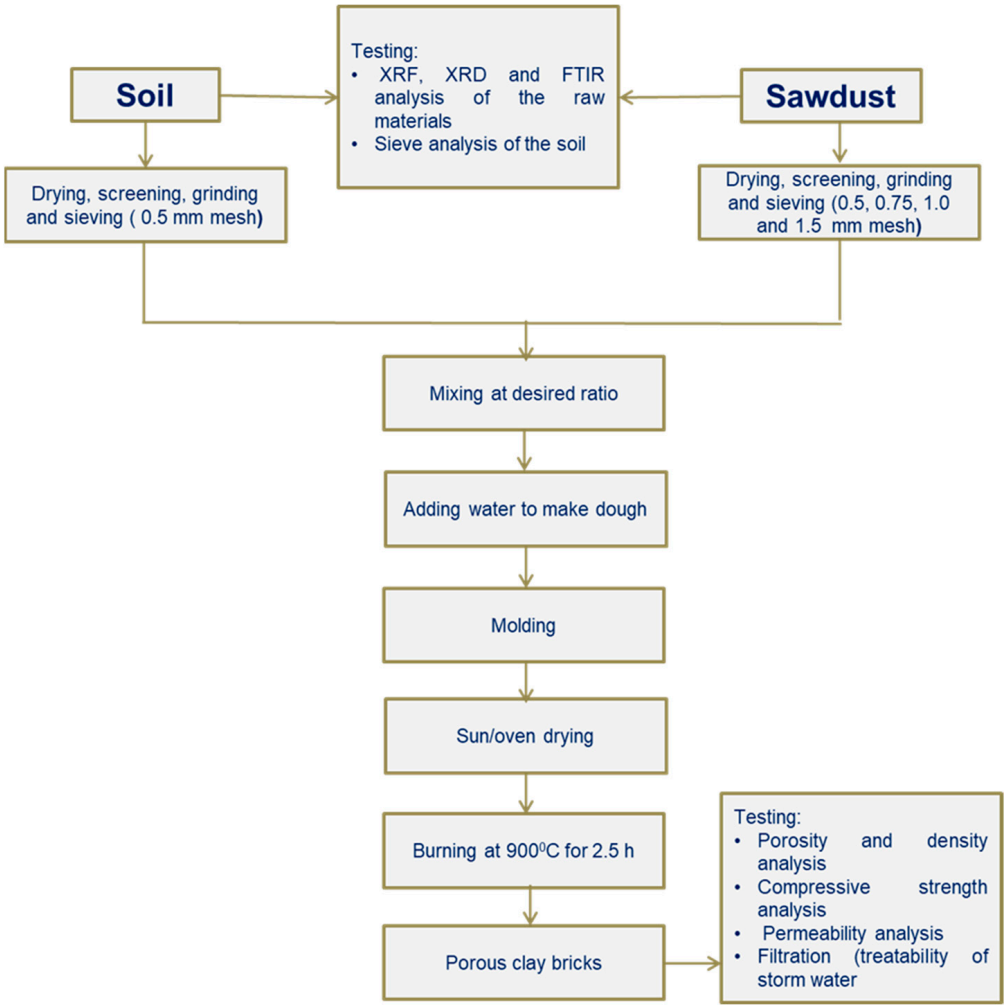

Figure 2. Flow chart of manufacturing procedure for porous bricks.

To optimize the size and ratio of SD in the brick's mixture, two series of bricks were prepared. Table 1 presents two series of bricks that were produced by mixing different ratios and sizes of SD with soil. In the first series, the bricks were made by mixing 0%, 5%, 10%, 15%, and 20% SD (by wt.) with soil. The produced bricks were named according to the % of SD in the mixture, as indicated in Table 1. For example, the bricks with 0% SD were named SD0, 5% SD as SD5, and so on. In the second series, the effect of the particle size of the SD on brick properties was investigated. In this series, 10% of selected sizes of SD were mixed with soil (see Table 1). The selected size of the SD was 0.5 mm (SD-0.5), 0.75 mm (SD-0.75), 1.0 mm (SD-1.0), and 1.5 mm (SD-1.5).

Figure 3. Laboratory procedure for porous clay bricks made of soil and sawdust for this study, (**a**) mixing soil and sawdust waste, (**b**) dough-making process by adding water, (**c**) casting dough into a wooden mold, (**d**) bricks after sun/oven drying, (**e**,**f**) bricks after completing the baking process.

Table 1. Bricks made by different ratios of sawdust with soil.

	Brick Name	SD Size (mm)	Soil (% by wt.)	SD (% by wt.)
Series 1	SD0	1.0	100	0
	SD5		95	5
	SD10		90	10
	SD15		85	15
	SD20		80	20
Series 2	SD-S0.5	0.5	90	10
	SD-S0.75	0.75	90	
	SD-S1.0	1.0	90	
	SD-S1.5	1.5	90	

2.3. Characterization of Raw Soil and Sawdust

2.3.1. Sieve Analysis of Soil

To classify the soil and its characteristics, sieve analysis was performed according to the methods described by ASTM D422-63 [39]. The percentage of each size of grain in the soil sample was determined from the cumulative grain size distribution curve. The sieve analysis was performed using sieves which had a mesh size of 1.18, 0.6, 0.5, 0.425, 0.3, 0.25, 0.18, 0.15, and 0.075 mm.

2.3.2. Chemical and Morphological Characterization of Soil and Sawdust

The elemental analyses of the soil and SD samples were conducted using the X-ray Fluorescence (XRF) technique. The crystalline structure of the soil and SD samples were analyzed through the X-ray diffraction technique (XRD) using ULTIMA IV/Rigaku(Rigaku, TX, USA) The main mineral phases of the samples were identified by the phase analysis of the samples using XRD methods. The sweeping speed of the samples was maintained at 1°/min between 2θ = 0° and 60°. The Fourier-transform infrared (FT-IR) spectrometer (Bruker Tensor 27 FTIR spectrometer) was used to obtain the infrared absorption spectra of the raw materials. The samples were thoroughly scanned between the wave number of 4000 and 400 cm^{-1}.

2.4. Characterization of Raw Soil and Sawdust

After manufacturing, all of the bricks were tested to assess their structural, mechanical, and hydrological properties for their possible application in permeable pavements. The tests included compressive strength, porosity, water adsorption, bulk density, permeability, and filtration capability. The details of the testing procedure of each parameter are presented in the subsequent sub-sections.

2.4.1. Apparent Porosity, Water Adsorption, and Bulk Density

The water boiling method described by ASTM C20-00 [40] was followed to determine the apparent porosity, water adsorption, and bulk density of the bricks. Initially, the brick samples were oven dried at 110 °C for 24 h, while the volume (V) and weight (D) were measured using a digital balance. The samples were then boiled with distilled water for 2 h. Following this, the samples were taken out to cool until reaching room temperature. Subsequently, the saturated mass (W) of the samples was measured. The following equations were used to calculate these three parameters:

$$\text{Porosity, } \% = \frac{W - D}{V} \times 100 \quad (1)$$

$$\text{Water adsorption, } \% = \frac{W - D}{D} \times 100 \quad (2)$$

$$\text{Bulk density, } \% = \frac{D}{V} \times 100 \quad (3)$$

2.4.2. Compressive Strength Tests

Compressive strength is one of the important properties that assess the brick's load-carrying capability. The method described by ASTM C67-05 [41] was employed to measure the compressive strength using the Universal Testing Machine (UTM). For the test, the brick specimens were fixed between the two pressing discs fitted in the machine and pressed to the complete failure (breakage) of the brick. The maximum pressures at failure, as well as the pressure distribution, were recorded in the computer connected to the UTM machine. The compressive strengths were then calculated using the following equation:

$$\text{Compressive strength , } M = \frac{\text{Maximum applied load, } P\ (N)}{\text{Surface area, } A\ (mm^2)} \quad (4)$$

2.4.3. Permeability Test

The standard falling head method described by ASTM D2434-68 [42] was employed to measure the permeability coefficient of the bricks. The test was carried out with a plastic bucket. The test specimen was fixed at the bottom of the bucket using acryl glue and kept for 72 days for drying. Subsequently, the permeability test was initiated by filling the bucket with tap water to a height of (h1). The water was then allowed to pass through

the bricks, and the time required to reach the water height until h2 was recorded. The permeability coefficient was then calculated using Equation (5).

$$k = \frac{a \times l}{A \times t} \ln\left(\frac{h_1}{h_2}\right) \quad (5)$$

where k is the permeability coefficient (cm/s), a is the bucket cross-section area (cm^2), A is the cross-sectional area of the brick samples (cm^2), and l is the specimen thickness (cm).

2.4.4. Stormwater (Runoff) Filtration Experiments

The stormwater filtration experiments were carried out using the selected bricks (SD ratio 10%) to assess their pollutant-removal capability for stormwater and the potential for practical field applications. The test was performed simply using a plastic bucket (20 cm high and 20 cm diameter) with a hole at the bottom. The selected bricks were fixed at the bottom of the bucket with acryl glue. Figure 4 shows the photograph and details schematics of the laboratory-scale filtration experiments. The stormwater was poured into the plastic bucket, allowing it to gravitationally filtrate through the porous bricks. The stormwater used in this experiment was collected from a natural pond in Buriadah city, Al-Qassim, Saudi Arabia. All of the samples were collected in high-density polyethylene (HDPE) bottles and stored at 4 °C. The pH, DO, and BOD_5 tests of the samples were performed within 48 h of collection. The filtration tests were carried out continuously for three days, and the quality of the filtrated water was analyzed on a daily basis.

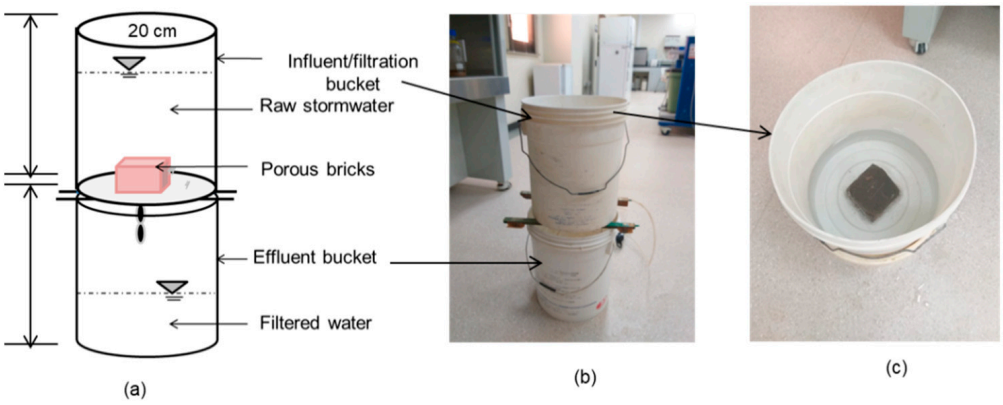

Figure 4. Filtration experiments, (**a**) schematics of filtration experiments, (**b**) laboratory picture of filtration experiments, and (**c**) top view of filtration bucket.

2.5. Water Quality Analysis

The water quality of both the raw stormwater and filtered water was analyzed following the standard methods defined by the American Public Health Association (APHA) [43]. The electrical conductivity (EC), pH, and dissolved oxygen (DO) were determined using a portable pH, EC, and DO meter provided by Hach (HACH, Loveland, CO, USA). Turbidity was measured using a Hach 2100Q turbidity meter (2100Q, HACH, Loveland, CO, USA). The gravimetric method was followed for measuring the total suspended solids (TSS). The standard procedure described by the APHA [43] was employed to measure the Biochemical Oxygen Demand (BOD_5).

2.6. Statistical Analysis

A single-factor analysis of variance (ANOVA) test was performed to determine the statistical difference of the brick properties made of different mixing ratios (%) and particle sizes of SD. The test was carried out using Microsoft Excel analytical tools with a 95% confidence interval.

3. Results and Discussions

3.1. Grain Size Distributions of Soil

The characteristics and behavior of soil largely depend on geotechnical characteristics. The compressive strength, density, and water content have a significant impact on the particle size distribution of the soil. Therefore, the soil used to manufacture the porous bricks in this study was characterized by sieve analysis. According to the particle size distribution, soil can be grouped into clays (<0.002 mm), silts (0.002–0.075 mm), fine sands (0.075–0.42), medium sands (0.42–2.0 mm), and gravels (2.0–75 mm). The soil can behave quite differently within these five major groups. Moreover, the soil grading can be defined by calculating the uniformity coefficient (Cu) and the coefficient of curvature (Cc). Soil is classified as well graded if the Cu value is more than 4. The soil classifies poorly or uniformly graded at Cu values less than 4, and Cc values ranging between 1 and 3 classify the soil as well graded. Compared to well-graded soils, poorly-graded soils are more vulnerable to soil liquefaction. The grain size distribution of the soil was calculated based on the sieve analysis, and the results are presented in Table 2. It was observed that the soil contains 18.8% of medium-size sand, 63.7% of fine sand, and 17.5% of clay/silt. Based on this size distribution, the soil can be classified as sandy clay soil.

Table 2. Characteristics of the selected soil based on the sieve analysis results.

Soil Characteristics	Values
D10	0.06
D30	0.14
D60	0.22
Cu	3.67
Cc	1.48
Gravel (%)	0.0
Medium sand (%)	18.8
Fine sand (%)	63.7
Clay/silt (%)	17.5

The values of Cu (3.67) and Cc (1.48) in the soil sample indicated that the values are at the boundary of well-graded (Cu > 4, Cc = 1−3) and poorly graded (Cu < 4, Cc < 1). Therefore, the soil can be defined as medium to fine mixed-graded soils.

3.2. Elemental Compositions of Soil and SD Samples

Table 3 presents the chemical compositions of the soil and SD samples measured by the XRF technique. The soil sample contains a suitable amount of SiO_2 (50.47%) and Al_2O_3 (19.14%), which are within the normal values (50–60% SiO_2 and 10–20% Al_2O_3) and considered to be appropriate for normal clay brick manufacturing [38]. More than 60% of SiO_2 may increase the porosity of the bricks. On the contrary, if the Al_2O_3 amount in the soil is more than 20%, it may decrease the compressive strength of the bricks [38]. Other fluxing agents such as Fe_2O_3, CaO, and MgO were present in the soil, and their total proportion was 15.34%. The results indicated that the soil is a low refractory material, i.e., these fluxing agents in the soil help to lower the melting point of the bricks during the baking process [38]. The existence of less than 6% CaO (3.2%) indicates that the soil is non-calcareous [38]. The SD sample contents were 33.11% SiO_2, 16.38% Al_2O_3, 9.56% Fe_2O_3, and a relatively higher amount (28.08%) of CaO. Therefore, the SD sample is categorized as calcareous and has more refractory materials.

Table 3. Chemical compositions of soil and SD based on XRF analysis.

Compositions (%)	Soil	SD
Silica (SiO_2)	50.47	33.11
Alumina (Al_2O_3)	19.14	16.38
Iron oxide (Fe_2O_3)	8.87	9.56
Calcium oxide (CaO)	3.2	28.08
Magnesium oxide (MgO)	3.27	0
Others	11.05	12.87

3.3. FTIR Analysis of Raw Soil and SD Samples

Figure 5 shows the FTIR spectra of the soil and SD samples. For the soil, the bands at 1084 cm^{-1}, 741 cm^{-1}, 699 cm^{-1}, and 471 cm^{-1} indicated that the soil is quartz-rich. The intense peaks in the region of wavenumber 800–400 cm^{-1} belong to feldspar, consisting of aluminosilicates of potassium, sodium, and calcium [44]. The absorption bands at 983 cm^{-1} in the soil samples possibly indicated the existence of sulfates in the samples [45]. The distinct vibration bands at 741 cm^{-1} identified the existence of dolomite in the soil samples [46]. The FTIR spectra of the carbonates were found at 1790–1820 cm^{-1} and 1400–1500 cm^{-1}, 870 cm^{-1}, and 741 cm^{-1} [46]. The vibrations observed at 440–400 cm^{-1} support the presence of hematite consisting of ferric oxide [46]. The absorption bands at 3688, 3624, 3615, 905, 699, and 471 cm^{-1} clearly specified the presence of kaolinite in the samples [44]. The absorption spectra at 471 cm^{-1} signify the presence of Si-O [45]. The distinct spectra in the area 1640–1600 cm^{-1} were due to the presence of OH-adsorbed water [45] or due to the presence of magnesium-rich chlorite in both samples. The clear bands between 3400 and 3750 cm^{-1}, observed in the soil sample, can be attributed to hydroxyl linkage (O–H) [45].

For the SD samples, a broad vibration band was observed at 3291 cm^{-1}, indicating the presence of cellulose and lignin phenol clusters in the samples [47]. The vibration band at 2850 cm^{-1} was due to the uneven vibrations of—CH_2 and—CH_3. The peak at 1587 cm^{-1} indicated the presence of a carboxylate cluster in the SD samples. The vibration band at 1328 cm^{-1} shows the presence of pectin (-COOH). The peak at 1213 cm^{-1} signifies hemicellulose vibration. The presence of the halogen group C-X in the SD sample is identified by the vibration bands observed at 1011 cm^{-1} and 1042 cm^{-1} [48].

3.4. XRD Analysis of Raw Soil and SD Samples

Figure 6 presents the X-ray diffraction patterns of the soil and SD samples. The interplanar spacing corresponding to XRD peaks observed for the clay soil-1 sample shows the presence of quartz (Q), dolomite (D), kaolinite (K), calcite (C), and feldspar (F), illite (I), and chlorite (ch). The results of XRD are consistent with the findings of the FTIR spectra. The X-ray diffraction patterns of the raw SD samples showed two distinct diffraction peaks around $2\theta = 16^\circ$ and 22°, indicating that the SD contains both amorphous and crystalline cellulose [49].

3.5. Properties of Bricks with Varying Percentages of Sawdust

Figure 7 presents the compressive strength, bulk density, porosity, and water adsorption of bricks made of soil with varying percentages of SD. The results showed that compressive strength and bulk density significantly decreased ($p > 0.005$) as the % of SD increased in the brick specimens. In contrast, the apparent porosity and water adsorption capacity significantly increased ($p < 0.005$) with the increase in the percentage of SD. With an increase in SD% from 0% to 20%, the compressive strength decreased from 26.8 to 7.6 MPa and the bulk density from 2.01 to 1.25 g/m^3. On the contrary, the corresponding increase in apparent porosity and water adsorption ranged from 7.4% to 56.7% and 3.7% to 45.4%, respectively. The inter-particle bond between the clay particles destabilized with the increase in SD in the clay mixture, which decreased the bulk density and compressive strength of the bricks [50]. Furthermore, the organics present in the SD were completely

burnt out during the firing process at 900 °C, which generates pores in the brick's structure [51]. Consequently, the porosity and the water adsorption of the bricks increases when increasing the SD% in the soil mixture, as presented in Figure 7.

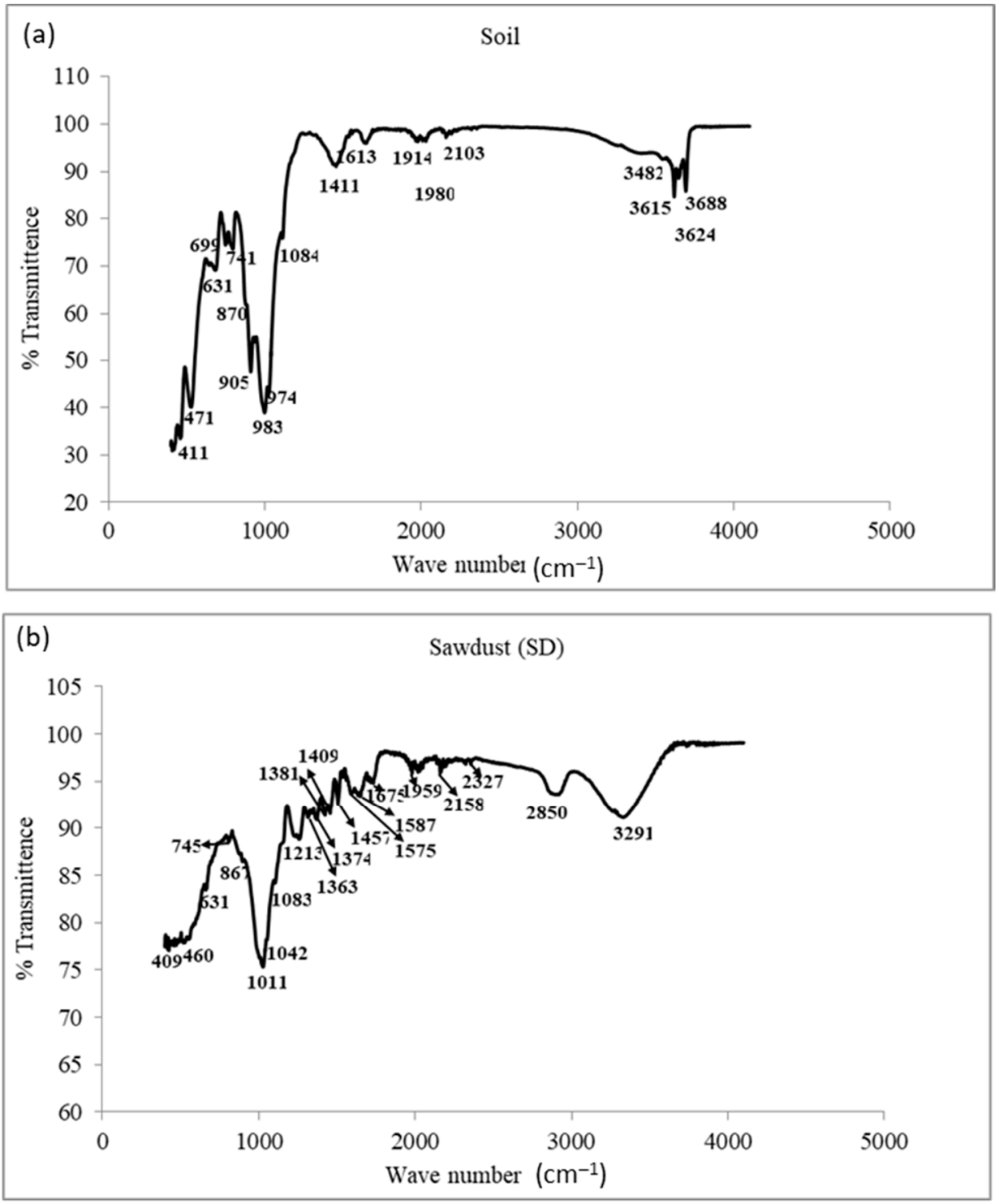

Figure 5. FTIR spectra for raw (**a**) soil and (**b**) sawdust samples.

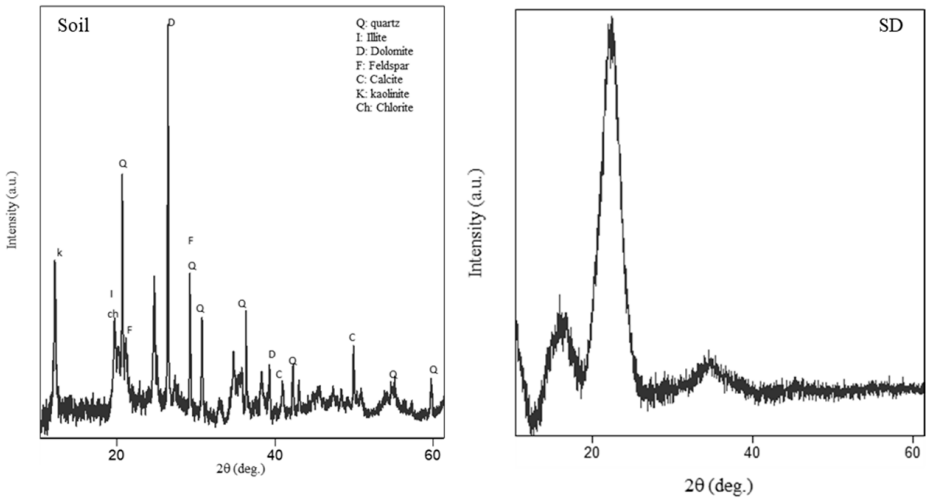

Figure 6. X-ray diffractogram of soil and SD samples.

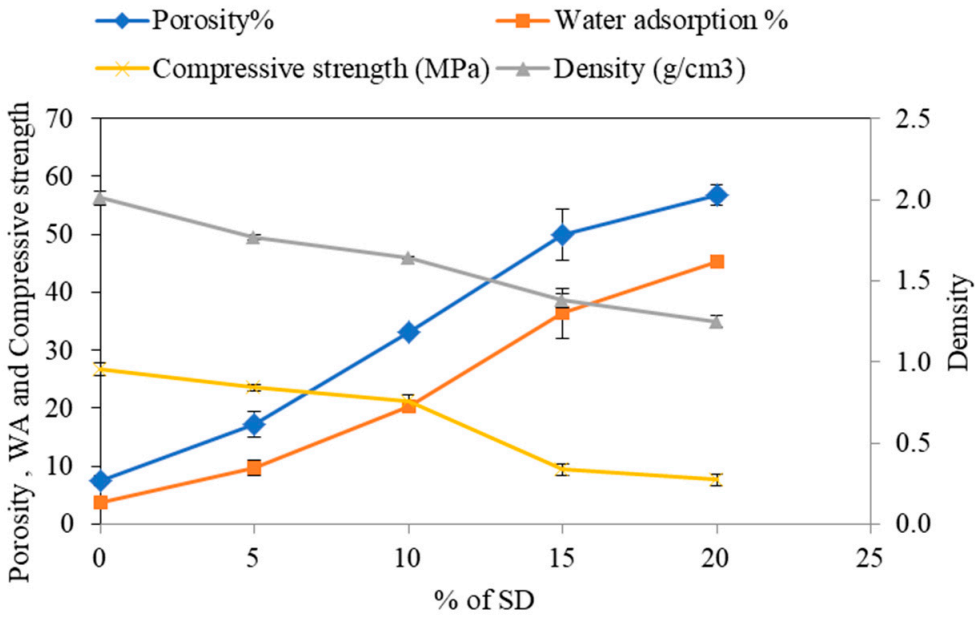

Figure 7. Compressive strength, bulk density, porosity, and water adsorption of bricks made of soil with varying % of SD.

Figure 8 further correlates the experimental data of the measured brick properties to provide insights into the brick performance. A strong positive relation was found between water adsorption and porosity (R^2 = 0.983) as well as between the compressive strength and bulk density (R^2 = 0.942). On the contrary, the strong negative correlation of compressive strength with the water adsorption (R^2 = 0.968) and apparent porosity (R^2 = 0.941) indicated that the SD% in the soil mixture needs to be optimized to balance these properties in permeable bricks. Our data indicated that with 10% SD, the bricks archived sufficient compressive strength (21.28 MPa), water adsorption (20.27%), and porosity (33.23%) to meet the standards for pedestrian and light traffic paving bricks (ASTM C 902) [52]. It is worth mentioning that the standard value of the brick's compressive strength for severe weather and moderate weather conditions is ≥17.2 MPa (2500 Psi) [52]. Thus, 10% SD with a 90% soil mixture by weight was selected as the optimum ratio for permeable clay bricks in this study.

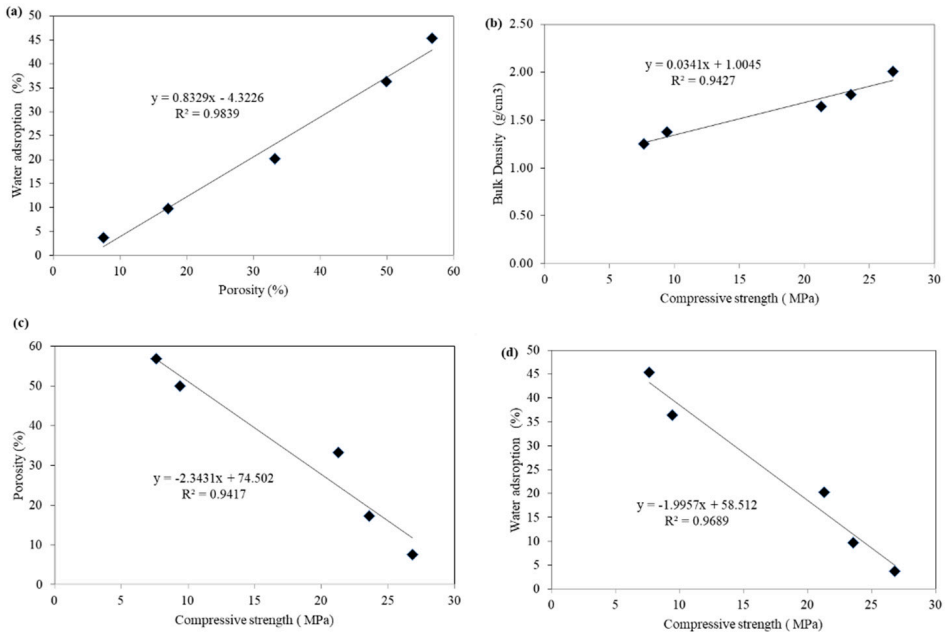

Figure 8. Correlation between different properties of bricks made of varying % of SD (**a**) water adsorption and porosity, (**b**) bulk density and compressive strength, (**c**) porosity and compressive strength, and (**d**) water adsorption and compressive strength.

In a further study, the effect of SD size in the clay was also investigated and the results are presented in Figure 9. It was observed that with a 10% ratio, the SD sizes from 0.5 mm to 1.0 mm did not significantly ($p < 0.05$) affect the brick's compressive strength and bulk density. However, the compressive strength and bulk density were significantly reduced when the SD size increased to 1.5 mm, and they did not meet the ASTM paving specifications [52]. On the contrary, the porosity and water adsorption were increased at 1.5 mm SD. For large SD sizes, the porosity of the bricks increased, which decreased the compressive strength. Therefore, the study results suggest that an SD size of <1 mm is appropriate for permeable brick manufacturing.

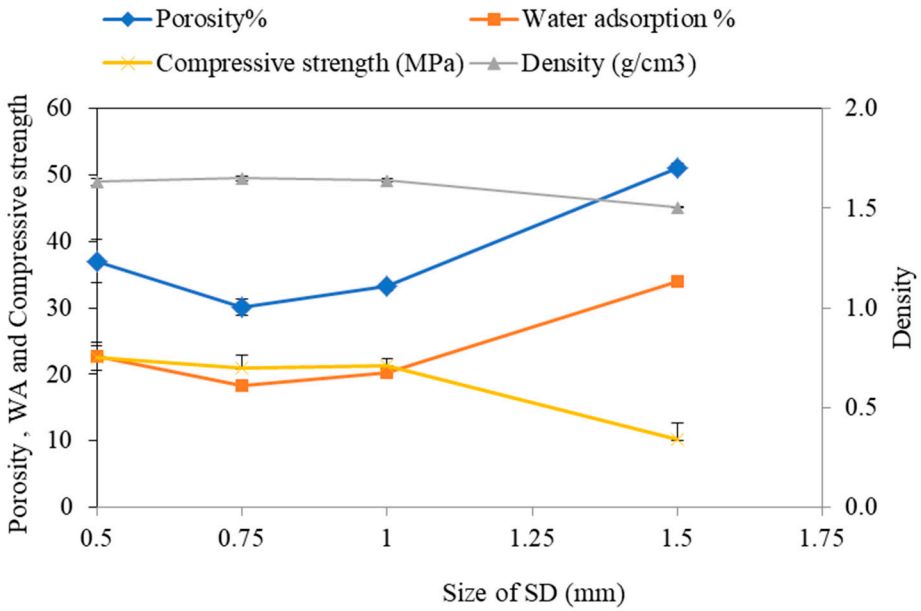

Figure 9. Compressive strength, bulk density, porosity, and water adsorption of bricks made of soil with varying sizes of SD.

3.6. The Permeability Coefficient of Bricks Made of Soil with Varying % and Size of SD

The permeability coefficient is one of the key parameters that provide insight into the stormwater filtration rate of permeable bricks. The permeability coefficient as a function of SD% is presented in Figure 10. As the SD% increased, the permeability coefficient increased significantly ($p > 0.05$). The permeable coefficient increased from 0.0010 cm/s up to 0.071 cm/s as the SD % increased from 0 to 20% in the soil mixture. The permeability coefficient was achieved to 0.0556 cm/s at 10% SD, which is significantly higher than the typical values for fully pervious pavements. For fully pervious pavements, the values of coefficient of permeability are greater than 0.01 cm/s, and for semi-pervious pavements, the values range between 0.01 and 0.0001 cm/s [53]. Therefore, the permeability coefficient values obtained in this study suggest the use of bricks with 10% SD in the permeable pavements.

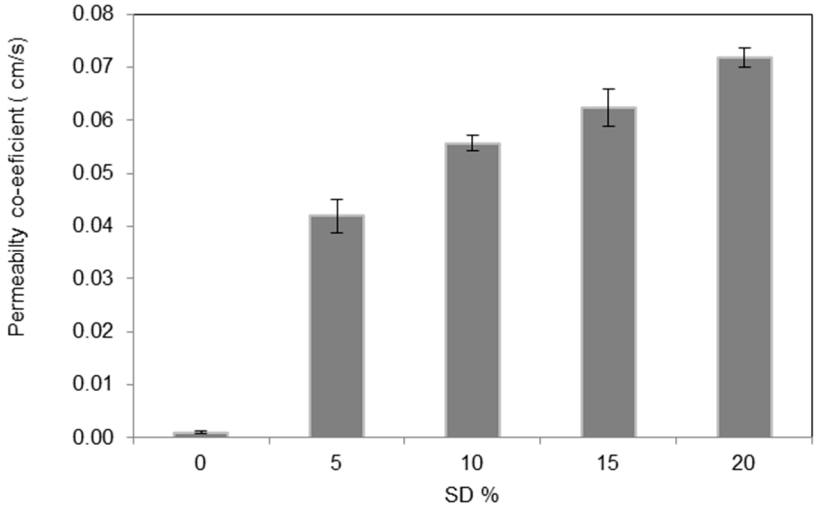

Figure 10. Permeability coefficients of bricks made of soil with varying % of SD.

Figure 11 illustrates the correlation of the permeability coefficient with the compressive strength and porosity. Positive correlations of the permeability coefficient with both compressive strength and porosity were observed with R^2 values of 0.68 and 0.82, respectively. The results indicated that the permeability increased when increasing the porosity.

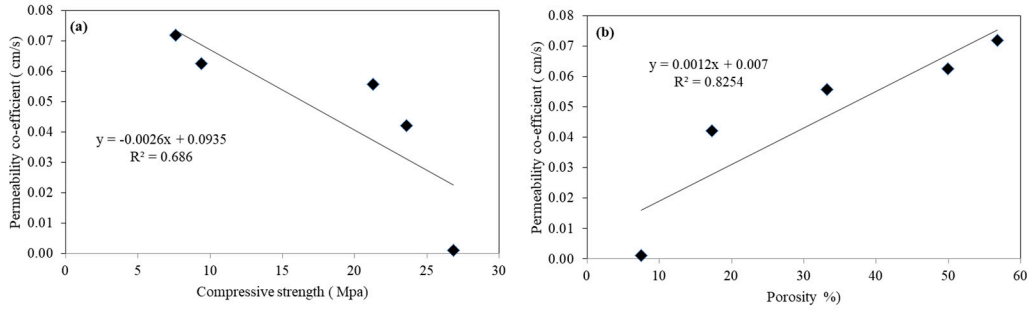

Figure 11. Correlation between permeability coefficient and (**a**) compressive strength, and (**b**) porosity.

Furthermore, the effect of the SD size on the permeability coefficient of the bricks was investigated, and the results are presented in Figure 12. The permeability coefficient gradually increased from 0.055 cm/s to 0.078 cm/s as the size of SD increased from 0.5 to 1.5 mm. All of these values of the permeability coefficient are well above the range of pervious pavements [53]. However, the compressive strength of the bricks made of 1.5 mm SD was significantly reduced and reached 10.2 MPa (Figure 12), which was incompatible with the standard of permeable bricks [52]. Thus, a size of SD up to 1 mm for manufacturing permeable clay bricks is recommended.

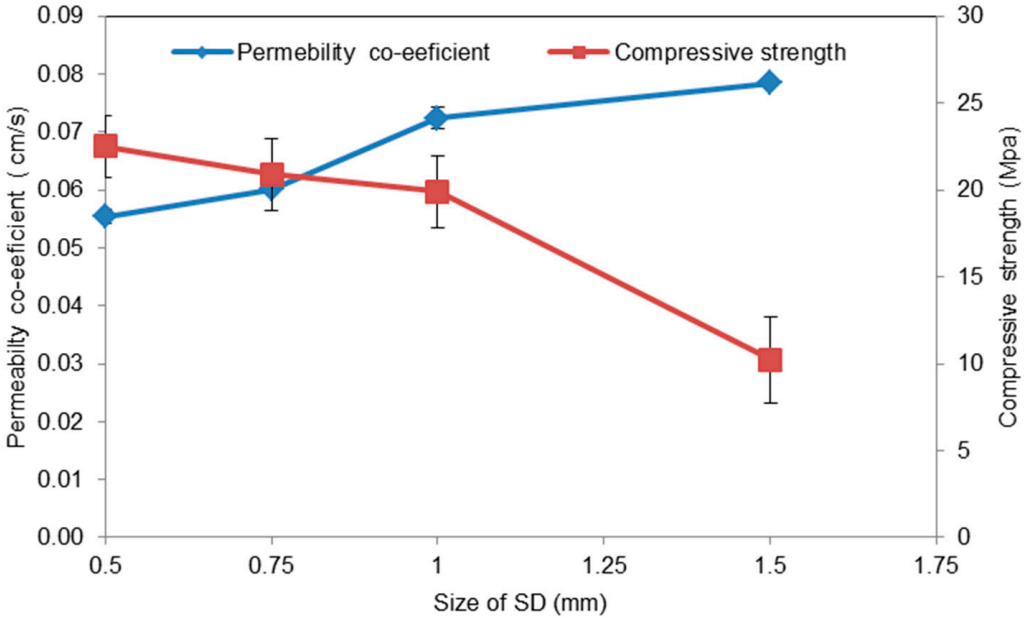

Figure 12. Permeability coefficients of bricks made of soil with varying sizes of SD.

Finally, the compressive strength and permeability coefficient of the bricks were compared with the standard for permeable paving bricks in Table 4. The results presented in Table 4 describe that the batch of bricks made by soil with SD (ratio 0–10% and size 0.5–1.0 mm) achieved the desired compressive strengths and permeability coefficient standards for potential application in PPS. Hence, it is recommended that the bricks made of 10% SD with a particle size of ≤1.0 mm and a 90% soil mixture (SD10) are suitable to make permeable clay bricks.

Table 4. Permeability coefficients of bricks made of soil with varying % and size of SD. All results are the average values of 3 brick specimens.

Brick Specimens	Soil (%)	SD (%)	SD SIZE (mm)	Permeability Coefficient (cm/s)	Compressive Strength (MPa)	Meet the Standards (Y/N)
SD0	100	0	1.00	0.0010	26.8	N
SD5	95	5	1.00	0.0420	23.6	Y
SD10	90	10	1.00	0.0556	21.2	Y
SD15	85	15	1.00	0.0624	9.4	N
SD20	80	20	1.00	0.0718	7.6	N
SD-S0.5	90	10	0.50	0.0554	22.5	Y
SD-S0.75	90	10	0.75	0.0601	20.8	Y
SD-S1.0	90	10	1.00	0.0724	19.8	Y
SD-S1.5	90	10	1.50	0.0785	10.2	N

3.7. Stormwater Treatment Efficiency of Selected Bricks

The bricks with SD10 (optimum ratio) were selected to conduct the filtration experiments to assess the performance of removing contaminants from the stormwater. Table 5 shows the pollutant concentrations in the raw and filtered stormwater samples. While pH, DO, EC and TDS remained unchanged after filtration, and it can be concluded that the bricks were unable to remove the dissolved salts from stormwater. Nevertheless, the TDS level (416.2 mg/L) in the raw stormwater was well below the recommended value (2500 mg/L) provided by the World Health Organization [54] for the wastewater reuse applications of restricted and unrestricted irrigation, fire protection, and toilet flushing. The pH and DO values in the filtered water were 7.9 and 62 mg/L, respectively. The high removal efficiency of 98.6% resulted in less than 10 mg/L TSS in the filtrate (also see

Table 5). Likewise, the high (96.8%) turbidity removal resulted in less than 1 NTU in the filtered water. High removal of TSS and turbidity from the stormwater indicate that the clay bricks are efficient in removing the particulate (TSS) and colloidal (turbidity) matter from the stormwater by a physical straining process.

Table 5. Concentrations of various pollutants in the stormwater and after filtration by permeable clay bricks made of soil −2 with 10% SD of size 1.0 mm.

Parameters	Unit	Observed Values	After Filtration	Removal Efficiency (%)	Wastewater Reuse Standard of KSA [55]	Wastewater Reuse Standard of WHO [54]
pH	-	8.1	7.9	-	6.0–8.4	6.0–9.0
TSS	mg/L	549.7	7.9	98.6	10	-
EC	us/cm	595.7	548.0	8.1		-
DO	mg/L	6.7	6.2	7.2		-
Turbidity	NTU	34.5	1.1	96.8	5	5
TDS	mg/L	416.2	407.7	2.0	2500	2500
BOD5	mg/L	44	9.8	77.7	10	-
TN	mg/L	7.0	5.0	28.2	40	-
TP	mg/L	2.1	1.4	33.6	-	-

The organic removal performance of the clay bricks was assessed by measuring the influent and effluent BOD. BOD5 was found to be 44 mg/L in the raw stormwater, which was higher than the desired wastewater reuse standards. The BOD removal was moderate (68.5%) and achieved less than 15 mg/L in the filtered water. Although the biological activities did not occur during the filtration process due to a short filtration period (3 d), it is anticipated that the particulate fraction of the organics was removed by the physical straining and the dissolved fraction via adsorption onto the surface of the clay bricks [56]. Relatively low removal efficiencies of TN (28.2%) and TP (33.6%) were achieved. The filtrated water quality was compared with the standard guidelines for wastewater reuse given in Table 5. The results showed that all of the measured pollutants in the filtered water were well below the standard guidelines.

3.8. Comparison of the Key Properties of the Bricks between This Research and the Previous Studies

The brick quality and durability greatly depend on several factors, including the raw materials and their compositions (ratios). These factors significantly influence the density, porosity, water adsorption, as well as the strength of the bricks. A number of previous studies investigated the influence of the addition of waste materials on porous clay brick production. Table 6 summarizes the experimental results of previous studies that have been reported in the literature and compares them with the main findings of this study. It can be seen in the table that the results of the present study are comparable with previous studies. It is clear from most of the studies that the addition of waste materials to the mixture significantly increases water adsorption and porosity while it decreases compressive strength and density. Therefore, the finding of this study revealed that sawdust-incorporated clay bricks would be a sustainable material for permeable pavement applications.

Table 6. Comparison between the findings of previous studies and this research.

Waste Materials	Ratio (%)	Key Properties of the Bricks				References
		Density (g/cm^3)	Water Adsorption (%)	Porosity (%)	Compressive Strength (MPa)	
Sawdust	0–10	1.4–1.88	9.02–27.2	15.7–39.6	4.1–36.63	[57]
Fly ash	0–20	1.85–2.07	15.2–17.5	28–32.5	16–26	[58]
Sewage sludge	35–50	0.22–0.29	6–13.8	-	8.5–12.5	[59]
Residual Pulp	0–20	1.21–1.7	13–27	-	3–11.5	[60]
Rice husk	10	-	22–27	-	7–8	[61]
Glass waste	0–30	2.21–2.24	12.9–14.5	-	35.2–48.2	[62]
Water treatment sludge	0–20	0.74–0.97	51–91	50–67	3–18	[63]
Rice Bran	0–20	1.3–1.9	10.5–39.3	10.1–59.1	6.98–29.7	[50]
Sawdust	0–20	1.25–2.01	3.71–45	7.47–56	6.5–27.5	This study

4. Conclusions

In this study, permeable clay paving bricks made of soil and sawdust waste that can be used as the surface layer of permeable pavements were successfully developed. The soil used in this study contains a significantly higher % of clay/silt (17.5%) and appropriate amounts of SiO_2 (50.47%), Al_2O_3 (19.14%), and fluxing agents (15.34%) for clay brick manufacturing. The soil sample primarily comprised quartz, dolomite calcite, feldspar, illite, kaolinite, and chlorite. The SD sample was enriched with amorphous and crystalline cellulose and contained a higher % of Cao, and was categorized as calcareous and had more refractory materials. The mixture of soil and 10% SD (size 0.5–1.0 mm) achieved the desired compressive strength (21.2 MPa) and permeability coefficient (0.0556 cm/s), and it was selected as the optimal ratio for manufacturing the porous bricks. The compressive strength and bulk density decreased with the increasing % of SD in the brick specimens. In contrast, the apparent porosity, water adsorption, and permeability coefficient increased with the increasing % of SD. The size of SD between 0.5 and 1.0 mm did not significantly ($p < 0.05$) change the compressive strength of the bricks suggested for use at these sizes for brick manufacturing. The total suspended solids (TSS), turbidity, and BOD_5 from the stormwater were effectively removed to below the standard limit set by the WHO for wastewater reuse applications. The developed porous clay bricks can be applied as the surface layer of permeable pavements as a viable stormwater management option in the urban areas of arid and semiarid regions. Further study is recommended to test the feasibility of these bricks by conducting field experiments with real permeable pavement layers with their underlying structure.

Author Contributions: Conceptualization, M.S. and S.M.A.A.; Data curation, H.H.; Formal analysis, M.S.; Funding acquisition, M.S.; Investigation, S.M.A.A., M.A. and F.A.; Methodology, M.S.; Project administration, M.S.; Resources, M.R.; Supervision, M.S.; Visualization, M.R.; Writing—original draft, M.S.; Writing—review & editing, H.H., M.R., M.A., F.A. and Y.E.-G. All authors have read and agreed to the published version of the manuscript.

Funding: This research was funded by the Deanship of Scientific Research, Qassim University, grant No.10184-qec-2020-1-3-I.

Institutional Review Board Statement: Not applicable.

Informed Consent Statement: Not applicable.

Data Availability Statement: Not applicable.

Acknowledgments: The authors gratefully acknowledge Qassim University, represented by the Deanship of Scientific Research, for the financial support for this research under the number (10184-qec-2020-1-3-I) during the academic year 1442 AH/2020 AD.

Conflicts of Interest: The authors declare no conflict of interest.

References

1. Ghumman, A.R.; Ghazaw, Y.M.; Alodah, A.; Rauf, A.U.; Shafiquzzaman, M.; Haider, H. Identification of Parameters of Evaporation Equations Using an Optimization Technique Based on Pan Evaporation. *Water* **2020**, *12*, 228. [CrossRef]
2. Brabec, E.; Schulte, S.; Richards, P.L. Impervious surfaces and water quality: A review of current literature and its implications for watershed planning. *J. Plan. Lit.* **2002**, *16*, 499–514. [CrossRef]
3. Newman, A.P.; Aitken, D.; Antizar-Ladislao, B. Stormwater quality performance of a macro-pervious pavement car park installation equipped with channel drain based oil and silt retention devices. *Water Res.* **2013**, *47*, 7327–7336. [CrossRef] [PubMed]
4. Brattebo, B.O.; Booth, D.B. Long-term stormwater quantity and quality performance of permeable pavement systems. *Water Res.* **2003**, *37*, 4369–4376. [CrossRef]
5. Haider, H.; Ghumman, A.R.; Al-Salamah, I.S.; Ghazaw, Y.; Abdel-Maguid, R.H. Sustainability evaluation of rainwater harvesting based flood risk management strategies: A multilevel decision-making framework for arid environments. *Arab. J. Sci. Eng.* **2019**, *10*, 8465–8488. [CrossRef]
6. Mugume, S.N.; Gomez, D.E.; Fu, G.; Farmani, R.; Butler, D. A global analysis approach for investigating structural resilience in urban drainage systems. *Water Res.* **2015**, *81*, 15–26. [CrossRef]
7. Bhatt, A.; Bradford, A.; Abbassi, B.E. Cradle to- grave life cycle assessment (LCA) of low-impact development (LID) technologies in southern Ontario. *J. Environ. Manag.* **2019**, *231*, 98–109. [CrossRef]
8. Qin, Y. Urban flooding mitigation techniques: A systematic review and future studies. *Water* **2020**, *12*, 3579. [CrossRef]
9. Zhang, P.; Chen, L.; Hou, X.; Wei, G.; Zhang, X.; Shen, Z. Detailed quantification of the reduction effect of roof runoff by low impact development practices. *Water* **2020**, *12*, 795. [CrossRef]
10. Hunt, W.F.; Traver, R.G.; Davis, A.P.; Emerson, C.H.; Collins, K.A.; Stagge, J.H. Low impact development practices: Designing to infiltrate in urban environments. In *Effects of Urbanization on Groundwater: An Engineering Case-Based Approach for Sustainable Development*; American Society of Civil Engineers: Reston, VA, USA, 2010; pp. 308–343.
11. Locatelli, L.; Mark, O.; Mikkelsen, P.S.; Arnbjerg-Nielsen, K.; Deletic, A.; Roldin, M.; Binning, P.J. Hydrologicimpact of urbanization with extensive storm water infiltration. *J. Hydrol.* **2017**, *544*, 524–537. [CrossRef]
12. USEPA. Green Infrastructure in the Semi-Arid West, Low-Impact Development and Green Infrastructure in the Semi-Arid West. Available online: https://www.epa.gov/green-infrastructure/green-infrastructure-semi-arid-west#6 (accessed on 20 November 2020).
13. Antunes, L.N.; Ghisi, E.; Thives, L.P. Permeable pavements life cycle assessment: A literature review. *Water* **2018**, *10*, 1575. [CrossRef]
14. Mullaney, J.; Lucke, T. Practical Review of Pervious Pavement Designs. *CLEAN Soil Air Water* **2013**, *42*, 111–124. [CrossRef]
15. Zhang, K.; Yong, F.; McCarthy, D.T.; Deletic, A. Predicting long term removal of heavy metals from porous pavements for stormwater treatment. *Water Res.* **2018**, *142*, 236–245. [CrossRef]
16. Pagotto, C.; Legret, M.; Le Cloirec, P. Comparison of the hydraulic behaviour and the quality of highway runoff water according to the type of pavement. *Water Res.* **2000**, *34*, 4446–4454. [CrossRef]
17. Rushton, B. Low-impact parking lot design reduces runoff and pollutant loads. *J. Water Resour. Plan. Manag.* **2000**, *127*, 172–179. [CrossRef]
18. Shafiquzzaman, M.; Alqarawi, S.M.A.; Haider, H.; Rafiquzzaman, M.; Almoshaogeh, M.; Alharbi, F.; El-Ghoul, Y. Evaluating Permeable Clay Brick Pavement for Pollutant Removal from Varying Strength Stormwaters in Arid Regions. *Water* **2022**, *14*, 491. [CrossRef]
19. Han, S.; Yang, Y.; Liu, S.; Lu, M. Decontamination performance and cleaning characteristics of three common used paved permeable bricks. *Environ. Sci. Pollut. Res.* **2020**, *28*, 15114–15122. [CrossRef]
20. Fwa, T.F.; Lim, E.; Tan, K.H. Comparison of permeability and clogging characteristics of porous asphalt and pervious concrete pavement materials. *Transp. Res. Rec. J. Transp. Res. Board* **2015**, *2511*, 72–80. [CrossRef]
21. Chandrappa, A.K.; Biligiri, K.P. Pervious concrete as a sustainable pavement material—Research findings and future prospects: A state-of-the-art review. *Constr. Build. Mater* **2016**, *111*, 262–274. [CrossRef]
22. Drake, J.A.P.; Bradford, A.; Marsalek, J. Reviewof environmental performance of permeable pavementsystems: State of the knowledge. *Water Qual. Res. J.* **2013**, *48*, 203–222. [CrossRef]
23. Li, F.; Liu, Y.; Engel, B.A.; Chen, J.; Sun, H. Green infrastructure practices simulation of the impacts of landuse on surface runoff: Case study in Ecorse River watershed, Michigan. *J. Environ. Manag.* **2019**, *233*, 603–611. [CrossRef] [PubMed]
24. Dondi, M.; Guarini, G.; Raimondo, M.; Zanelli, C.; Fabbriche, D.D.; Agostini, A. Recycling the insoluble residue from titania slag dissolution (tionite) in clay bricks. *Ceram. Int.* **2010**, *36*, 2461–2467. [CrossRef]
25. Faria, K.C.P.; Gurgel, R.F.; Holanda, J.N.F. Recycling of sugarcane bagasse ash waste in the production of clay bricks. *J. Environ. Manag.* **2012**, *101*, 7–12. [CrossRef]
26. Bories, C.; Borredon, M.E.; Vedrenne, E.; Vilarem, G. Development of eco-friendly porous fired clay bricks using pore-forming agents: A review. *J. Environ. Manag.* **2014**, *143*, 186–196. [CrossRef]
27. Thalmaiera, G.; Cobîrzana, N.; Baloga, A.A.; Constantinescua, H.; Strezab, M.; Nasuia, M.; Neamtua, B.V. Influence of sawdust particle size on fired clay brick properties. *Mater. Constr.* **2020**, *70*, 338. [CrossRef]

28. Beal, B.; Selby, A.; Atwater, C.; James, C.; Viens, C.; Almquist, C. A Comparison of thermal and mechanical properties of clay bricks prepared with three different pore-forming additives: Vermiculite, wood ash, and sawdust. *Environ. Prog. Sustain. Energy* **2019**, *38*, 13150. [CrossRef]
29. Maza-Ignacio, O.T.; Jiménez-Quero, V.G.; Guerrero-Paz, J.; Montes-García, P. Recycling untreated sugarcane bagasse ash and industrial wastes for the preparation of resistant, lightweight and ecological fired bricks. *Constr. Build. Mater.* **2020**, *234*, 117314. [CrossRef]
30. Zhang, Q.; Li, Y.; Yu, C.; Qi, J.; Yang, C.; Cheng, B.; Liang, S. Global timber harvest footprints of nations and virtual timber trade flows. *J. Clean. Prod.* **2020**, *250*, 119503. [CrossRef]
31. Penna, I. *Understanding the FAO's Wood Supply from Planted Forests Projections*, 1st ed.; Centre for Environmental Management, University of Ballarat: Ballarat, Australia, 2010; Volume 2010.
32. Rominiyi, O.L.; Adaramola, B.A.; Ikumapayi, O.M.; Oginni, O.T.; Akinola, S.A. Potential Utilization of Sawdust in Energy, Manufacturing and Agricultural Industry; Waste to Wealth. *World J. Eng. Technol.* **2017**, *5*, 526–539. [CrossRef]
33. Mwango, A.; Kambole, C. Engineering Characteristics and Potential Increased Utilisation of Sawdust Composites in Construction—A Review. *J. Build. Constr. Plan. Res.* **2019**, *7*, 59–88. [CrossRef]
34. Chemani, B.; Chemani, H. Effect of adding sawdust on mechanical-physical properties of ceramic bricks to obtain lightweight building material. *Int. J. Mech. Aerosp. Ind. Mechatron. Manuf. Eng.* **2012**, *6*, 2521–2525.
35. Chemani, H.; Chemani, B. Valorization of wood sawdust in making porous clay brick. *Sci. Res. Essays* **2013**, *8*, 609–614.
36. Herek, L.C.S.; Hori, C.E.; Reis, M.H.M.; Mora, N.D.; Tavares, C.R.G.; Bergamasco, R. Characterization of ceramic bricks incorporated with textile laundry sludge. *Ceram. Int.* **2012**, *38*, 951–959. [CrossRef]
37. Xu, Y.; Yan, C.; Xu, B.; Ruan, X.; Wei, Z. The use of urban river sediments as a primary raw material in the production of highly insulating brick. *Ceram. Int.* **2014**, *40*, 8833–8840. [CrossRef]
38. Velasco, P.M.; Morales Ortíz, M.P.; Mendívil Giró, M.A.; Muñoz Velasco, L. Fired clay bricks manufactured by adding wastes as sustainable construction material—A review. *Constr. Build. Mater.* **2014**, *63*, 97–107. [CrossRef]
39. *ASTM D422-63*; Standard Test Method for Particle-Size Analysis of Soils. ASTM International: West Conshohocken, PA, USA, 2014. [CrossRef]
40. *ASTM C20-00*; Standard Test Methods for Apparent Porosity, Water Absorption, Apparent Specific Gravity, and Bulk Density of Burned Refractory Brick and Shapes by Boiling Water. ASTM International: West Conshohocken, PA, USA, 2000.
41. *ASTM C67-05*; Standard Test Methods for Sampling and Testing Brick and Structural Clay Tile. ASTM International: West Conshohocken, PA, USA, 2005.
42. *ASTM D2434-68*; Standard Test Method for Permeability of Granular Soils (Constant Head). ASTM International: West Conshohocken, PA, USA, 2006.
43. American Public Health Association (APHA). *Standard Methods for the Examination of Water and Wastewater*, 21st ed.; American Public Health Association: Washington, DC, USA, 2005.
44. Farmer, V.C. Transverse and Longitudinal Crystal Modes Associated with OH Stretching Vibrations in Single Crystals of Kaolinite and Dickite. *Spectrochim. Acta Part A Mol. Biomol. Spectrosc.* **2000**, *56*, 927–930. [CrossRef]
45. Jozanikohan, G.; Abarghooei, M.N. The Fourier transform infrared spectroscopy (FTIR) analysis for the clay mineralogy studies in a clastic reservoir. *J. Pet. Explor. Prod. Technol.* **2022**, *12*, 2093–2106. [CrossRef]
46. Ji, J.; Ge, Y.; Balsam, W.; Damuth, J.E.; Chen, J. Rapid identification of dolomite using a Fourier transform infrared spectrophotometer (FTIR): A fast method for identifying Heinrich events in IODP Site U1308. *Mar. Geol.* **2009**, *258*, 60–68. [CrossRef]
47. Akhouairi, S.; Ouachtak, H.; Addi, A.A.; Jada, A.; Douch, J. Natural Sawdust as Adsorbent for the Eriochrome Black T Dye Removal from Aqueous Solution. *Water Air Soil Pollut.* **2019**, *230*, 181. [CrossRef]
48. Rahman, N.U.; Ullah, I.; Alam, S.; Khan, M.S.; Shah, L.A.; Zekker, I.; Burlakovs, J.; Kallistova, A.; Pimenov, N.; Vincevica-Gaile, Z.; et al. Activated Ailanthus altissima Sawdust as Adsorbent for Removal of Acid Yellow 29 from wastewater: Kinetics Approach. *Water* **2021**, *13*, 2136. [CrossRef]
49. Zhang, M.; Zhang, S.; Chen, Z.; Wang, M.; Cao, J.; Wang, R. Preparation and Characterization of Superabsorbent Polymers Based on Sawdust. *Polymers* **2019**, *11*, 1891. [CrossRef] [PubMed]
50. Alharbi, F.; Almoshaogeh, M.; Shafiquzzaman, M.; Haider, H.; Rafiquzzaman, M.; Al-Ragi, A.; ElKholy, S.; Bayoumi, E.-S.A.; El-Ghoul, Y. Development of rice bran mixed porous clay bricks for permeable pavements: A sustainable LID technique for Arid Regions. *Sustainability* **2021**, *13*, 1443. [CrossRef]
51. Khoo, Y.C.; Johari, I.; Ahmad, Z.A. Influence of Rice Husk Ash on the Engineering Properties of Fired-Clay Brick. *Adv. Mater. Res.* **2013**, *795*, 14–18. [CrossRef]
52. *ASTM C902-15*; Standard Specification for Pedestrian and Light Traffic Paving Brick. ASTM International: West Conshohocken, PA, USA, 2015.
53. Mayne, P.W.; Christopher, B.R.; DeJong, J. *Manual on Subsurface Investigations*; Publication No. FHWA NHI-01-031; National Highway Institute, Federal Highway Administration: Washington, DC, USA, 2001; p. 305.
54. World Health Organization (WHO). Excreta and Greywater Use in Agriculture. In *Guidelines for the Safe Use of Wastewater Excreta and Greywater*; WHO: Geneva, Switzerland, 2006; Volume 4.
55. Ministry of Water and Electricity (MWE). *Technical Guidelines for the Use of Treated Sanitary Wastewater in Irrigation for Landscaping and Agricultural Irrigationl*; Ministry of Water and Electricity: Riyadh, Saudi Arabia, 2006.

56. Ogunmodede, O.T.; Adebayo, O.L.; Ojo, A.A. Enhancing adsorption capacity of clay and application in dye removal from wastewater. *Int. Lett. Chem. Phys. Astron.* **2014**, *39*, 35–51. [CrossRef]
57. Zhang, Z.; Wong, Y.C.; Arulrajah, A.; Horpibulsuk, S. A review of studies on bricks using alternative materials and approaches. *Constr. Build. Mater.* **2018**, *188*, 1101–1118. [CrossRef]
58. Yang, C.; Cui, C.; Qin, J.; Cui, X. Characteristics of the fired bricks with low-silicon iron tailings. *Constr. Build. Mater.* **2014**, *70*, 36–42. [CrossRef]
59. Zhou, W.; Yang, F.; Zhu, R.; Dai, G.; Wang, W.; Wang, W.; Guo, X.; Jiang, J.; Wang, Z. Mechanism analysis of pore structure and crystalline phase of thermal insulation bricks with high municipal sewage sludge content. *Constr. Build. Mater.* **2020**, *263*, 120021. [CrossRef]
60. Muñoz, P.; Letelier, V.; Zamora, D.; Morales, M.P. Feasibility of using paper pulp residues into fired clay bricks. *J. Clean. Prod.* **2020**, *262*, 121464. [CrossRef]
61. Gorhan, G.; Simsek, O. Porous clay bricks manufactured with rice husks. *Constr. Build. Mater.* **2013**, *40*, 390–396. [CrossRef]
62. Tang, C.W. Properties of fired bricks incorporating TFT-LCD waste glass powder with reservoir sediments. *Sustainability* **2018**, *10*, 2503. [CrossRef]
63. Lin, K.L.; Chang, J.C.; Shie, J.L.; Chen, H.J.; Ma, C.M. Characteristics of porous ceramics produced from waste diatomite and water purification sludge. *Environ. Eng. Sci.* **2012**, *29*, 436–446. [CrossRef]